

## Magnetic properties of MnBi prepared by rapid solidification

X. Guo, X. Chen, Z. Altounian, and J. O. Ström-Olsen

*Centre for the Physics of Materials, Department of Physics, McGill University, 3600 University Street,  
Montréal, Québec, Canada H3A 2T8*

(Received 10 January 1992; revised manuscript received 13 May 1992)

The magnetic properties of the low-temperature phase of MnBi, prepared by rapid solidification, have been measured in a pulsed field over the temperature range 80–625 K. The anisotropy field, obtained by the singular-point-detection technique, is found to increase with temperature and has a maximum value of 9 T at 530 K. A fit to the saturation-magnetization measurement gives a virtual Curie point of 775 K. The coercive field is fitted by a hybrid domain-wall-pinning theory which yields, at 300 K, a domain-wall energy of 15.6 erg/cm<sup>2</sup> and a wall thickness of 70 Å. Below 200 K, the presence of a ferrimagnetic phase is detected. Its critical field associated with spin reversal is a convex function of temperature having a maximum value of 8 T at 120 K.

### I. INTRODUCTION

The equiatomic compound MnBi has long been of interest because of the large magnetocrystalline anisotropy of its low-temperature phase (LTP)<sup>1</sup> and the favorable magneto-optical properties of its quenched high-temperature phase (QHTP).<sup>2,3</sup> However, the formation of pure single-phase MnBi is difficult by conventional means. Recently, Guo *et al.*<sup>4</sup> have successfully prepared the MnBi LTP in bulk quantities by rapid quenching from the melt, followed by a simple thermal treatment. The resultant product contains more than 95 wt. % of the LTP. To date there have been no direct measurements of the anisotropy field of LTP, and results published have shown that some magnetic properties of the MnBi phases vary with the method of preparation and subsequent heat treatment.<sup>5</sup> It is therefore of interest to measure the magnetic properties of the LTP of MnBi prepared by rapid solidification, and this is the aim of the present work. We report the temperature dependence of the saturation magnetization  $M_s$ , anisotropy field  $H_a$ , and coercive field  $H_c$ .

### II. EXPERIMENTAL METHODS

MnBi ingots were prepared by arc melting appropriate amounts of Bi (99.999% purity) and Mn (99.99% purity) under titanium gettered argon atmosphere. The amorphous ribbons were obtained by ejecting about 1 g of the melt from a quartz crucible onto the surface of a rotating copper wheel under argon atmosphere of about 30 kPa. The tangential speed of the wheel was 50±5 m/s and the nozzle diameter of the quartz tube was 0.25 mm. The ribbons were then compressed to form a cylinder 3.16 mm high and 3.28 mm in diameter. This specimen was heated at a rate of 80 K/min to 570 K to form LTP. X-ray (Cu  $K_\alpha$ ) diffraction showed the presence of a single LTP with a small amount of Bi (<5 wt. %), which we have corrected for in the magnetization measurements.

For magnetic measurements, a pulsed field of up to 18 T and a computer for collecting data were used. Signals

of  $dM/dt$ , the derivative of magnetization with respect to time, were generated by pick-up coils similar to the design of Allain *et al.*<sup>6</sup> Between the pick-up coil and the computer, an electronic integrator and a differentiator were used, respectively, for converting  $dM/dt$  to the magnetization  $M$  and its second derivative,  $d^2M/dt^2$ , which is required in the singular point detection (SPD) method<sup>7</sup> in order to determine the anisotropy field. For magnetization measurements, the background was stored in the computer and was later subtracted from the overall signal of the specimen. The error in magnetization measurements is within 5%, and the instrument field resolution is smaller than 0.12 T. The specimen temperature was stabilized within ±1 K during the measurements.

### III. RESULTS AND DISCUSSION

#### A. Saturation Magnetization $M_s$

Hysteresis loops were measured over the temperature range 80–600 K. Loops at several temperatures are shown in Fig. 1. The wider loop at higher temperature shows the increased coercivity that will be analyzed in Sec. III D.

Since the applied field, 18 T, is more than nine times larger than the coercivity  $H_c$ , the maximum magnetization in these loops is a very good approximation to saturation magnetization  $M_s$ . The  $M_s$  thus obtained is plotted versus temperature in Fig. 2. Though it is apparently inconsistent with a neutron diffraction result,<sup>8</sup> the magnitude as well as the temperature dependence of  $M_s$  agrees with two other measurements: the data measured by a vibrating sample magnetometer on single-crystal MnBi (Ref. 1), and that measured by the gradient method on polycrystalline MnBi.<sup>9</sup> At 300 K, the magnetic moment is 3.44±0.17 $\mu_B$  per Mn atom.

In the present work, the temperature dependence of  $M_s$  can be described by the expression

$$M_s(T) = M_s(0) \{ (1-p)[1 - B(T/T_c)^{3/2}] + p(1 - T/T_c)^{1/2} \}, \quad (1)$$

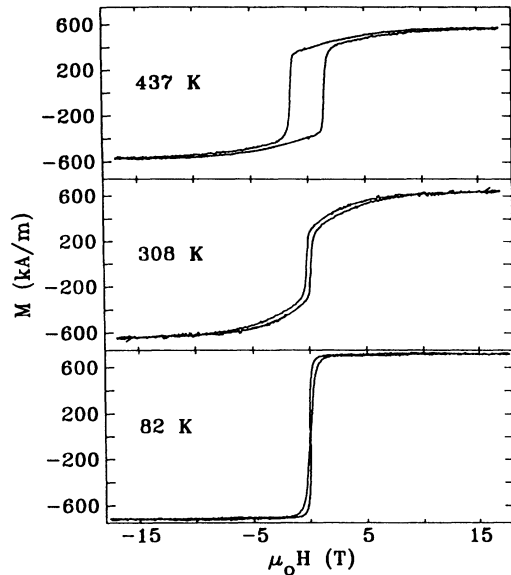


FIG. 1. Hysteresis loops of MnBi LTP at three temperatures.

where  $p = (T/T_c)^n$  is a weight function such that, at low and high temperatures, spin wave behavior,  $[1 - B(T/T_c)^{3/2}]$ , and critical point behavior,  $(1 - T/T_c)^{1/2}$ , are recovered, respectively.<sup>10</sup> Best fit to the data gives  $M_s(0) = 742$  kA/m,  $B = 0.4$ ,  $n = 1.25$ , and  $T_c = 775$  K. Since the LTP transforms to the high-temperature phase at 613 K,<sup>1</sup> the  $T_c$  thus obtained is a virtual one, and cannot be confirmed experimentally.

### B. Anisotropy field $H_a$

The easy magnetization direction of the LTP is reported to lie along the hexagonal  $c$  axis at room temperature,<sup>11,12</sup> and the present work confirmed this by the x-ray diffraction of a powder specimen aligned in field of 1T. An isotropic powder specimen was used to measure the anisotropy field over the temperature range 147–586 K by the SPD technique.<sup>7</sup> Figure 3 shows a set of SPD signals. The second derivative of magnetization with

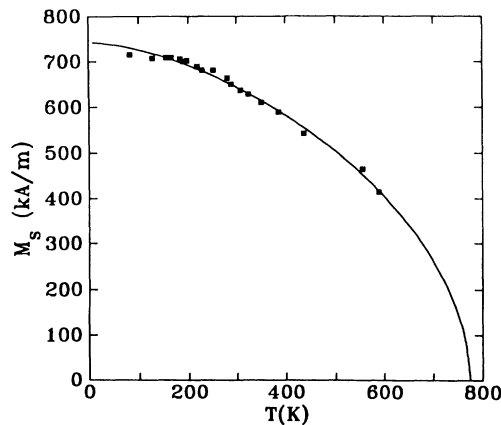


FIG. 2. Saturation magnetization of MnBi LTP at various temperatures. The square symbols represent the experiment data, and the solid line is calculated from Eq. (1)

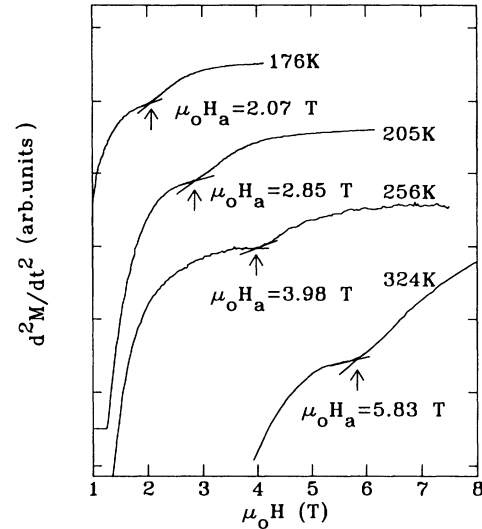


FIG. 3. Examples of SPD signals. The extrema in the  $d^2M/dt^2$  curves occur at the anisotropy field  $H_a$ .

respect to time,  $d^2M/dt^2$ , is plotted against magnetic field for various temperatures. The extrema in these curves are the singular points which occur at the anisotropy field,  $H_a$ .<sup>7</sup> Figure 4 shows the temperature dependence of the anisotropy field, which has the maximum value of 9 T at 514 K. The anisotropy constant<sup>7</sup>

$$K = K_1 + 2K_2 + 3K_3 = \mu_0 H_a M_s / 2 \quad (2)$$

is calculated from a polynomial fit to data for  $H_a$  and will be used in Sec. III D to calculate the domain wall energy and the wall thickness. Figure 5 shows the calculated anisotropy constant. Its magnitude as well as temperature dependence is consistent with that reported in Ref. 11, where the value of  $K_1 + K_2 + K_3$ , instead of  $K_1 + 2K_2 + 3K_3$ , is plotted.

### C. The spin reversal of HC

Below 200 K, an anomalous extremum was observed in the  $d^2M/dt^2$  curves, as shown in Fig. 6. The tempera-

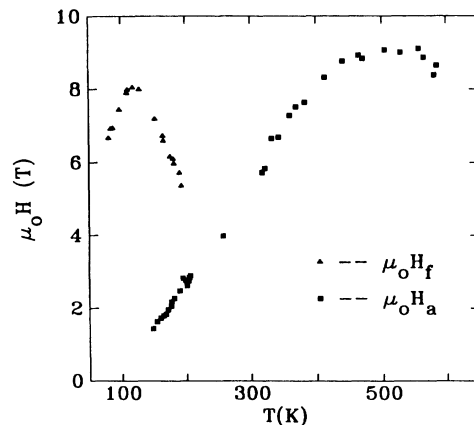


FIG. 4. Temperature dependence of  $\mu_0 H_a$ , the anisotropy field of LTP, and the critical field  $\mu_0 H_f$  of spin reversal in the HC phase.

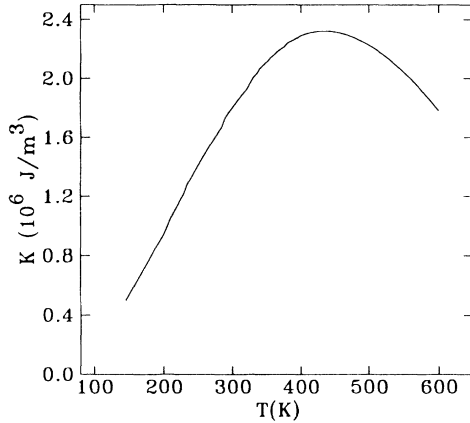


FIG. 5. Anisotropy constant  $K = K_1 + 2K_2 + 3K_3$  as a function of temperature.

ture dependence of the related critical field,  $H_f$ , is plotted in Fig. 4. This anomalous extremum is not associated with the anisotropy field, as is shown by the fact that it coexists with the extremum of  $H_a$  in the temperature range 145–200 K and is also much higher in value. The shape of the extremum is also different as may be seen by comparing Fig. 3 with Fig. 6. A possible explanation is that it may originate from a first-order magnetization process (FOMP).<sup>13</sup> However, using the data of reference,<sup>11</sup> the critical field of FOMP is estimated to be about 0.5 T, which is much lower than the observed  $H_f$  of between 5 and 8 T.

Notis *et al.*<sup>14</sup> and Pirich *et al.*<sup>15,16</sup> reported a metastable phase, HC, coexisting with LTP. This phase is crystallographically similar to the high-temperature phase (HT)  $\text{Mn}_{1.08}\text{Bi}$ , but has a much lower Curie temperature of 240 K. To explain the magnetic properties of the HC phase as ferrimagnetic, Pirich and co-workers<sup>15</sup> proposed the following model: since there are large vacancies in the two equivalent Bi sites (see Fig. 7), Mn ions may reside in these interstitial sites. The moments of these interstitial Mn ions are aligned antiparallel to that of the Mn ions on the main lattice sites. Thus, the HC phase is

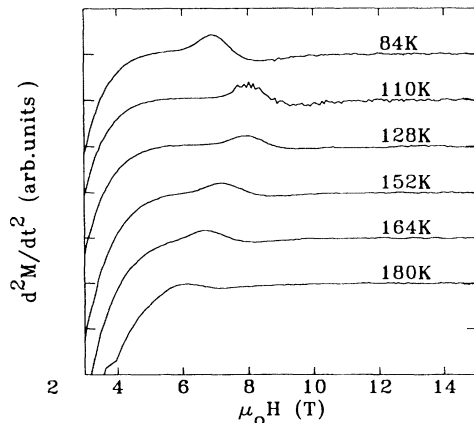


FIG. 6. Second derivatives,  $d^2M/dt^2$ , at various temperatures vs magnetic field, showing the signals originating from the spin reversal of the HC phase.

NiAs Structure  $P6_3/mmc$

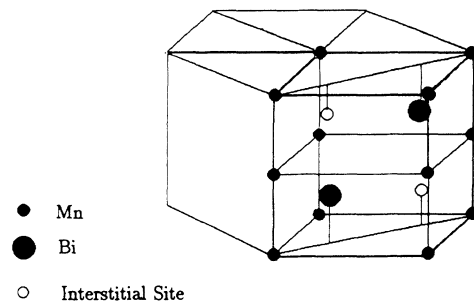


FIG. 7. A unit cell of MnBi, showing the two interstitial sites.

a defect crystallographic structure whose magnetic properties are dependent on interstitial site occupancy.<sup>15</sup> In the present work, the MnBi LTP is prepared by rapid solidification. The resulting specimen contains a small amount of Bi (< 5 wt. %), and it is possible that the extra Mn atoms occupy the interstitial sites to form the HC phase. From Fig. 4 the apparent ordering temperature (> 200 K) associated with  $H_f$  is close to the Curie temperature (240 K) of the HC phase; this provides further evidence for the presence of the HC phase. Since the moments of the Mn-lattice and Mn-interstitial ions are aligned antiparallel to each other along the easy  $c$  axis, it is expected that, similar to the spin-flopping observed in antiferromagnetic materials,<sup>17</sup> the spins of the interstitial Mn ions may reverse their orientation at some critical field to reduce the total energy. The critical field is expected to be much larger than the anisotropy field because the spin reversal in the HC phase is similar to spin flopping in antiferromagnetic materials, of which the critical field is  $(2H_m H_a)^{1/2}$ , where  $H_m$  is the molecular field.<sup>17</sup> Therefore, we conclude that the anomalous behavior in  $d^2M/dt^2$  originates from the spin reversal of the HC phase. To obtain further evidence, a specimen was annealed at 570 K for six days, and then measured by the SPD method. Annealing should reduce the number of interstitial Mn ions, and hence the amount of HC phase; and in fact, only signals associated with the anisotropy field were observed in the  $d^2M/dt^2$  curve of the annealed specimen, implying that the HC phase had indeed disappeared after such a thermal treatment. This result agrees with that observed by Pirich.<sup>16</sup>

#### D. Coercive field $H_c$

Figure 8 shows  $H_c$  values at different temperatures.  $H_c$  increases dramatically from 0.2 T at room temperature to 1.8 T at 500 K. Different models of domain nucleation and domain-wall pinning have been used to fit the data, but no single model is satisfactory. However, combining Hilzinger and Kronmüller's model of two-dimensional wall bowing<sup>18,19</sup> with Gaunt's consideration of thermal activation,<sup>20,21</sup> produces hybrid model which fits the data satisfactorily.

Prior to the description of the hybrid domain-wall-

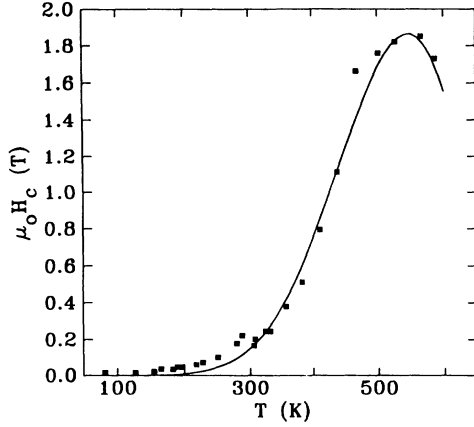


FIG. 8. The coercive field  $H_c$  of LTP prepared by rapid solidification. The square symbols are the experiment data, and the solid line is a fit to the hybrid wall pinning model.

pinning model, it is necessary to estimate the maximum pinning force  $f$  between one pinning site and a domain wall. Following the general convention,  $\pi\delta$  denotes the domain-wall thickness and  $\gamma$  denotes wall energy per unit area. The orientations of atomic moments inside a domain wall deviate from easy direction and from each other. The former gives the wall an anisotropy energy increment represented by  $K$ ; and the latter gives an exchange energy increment represented by  $A$ .  $A$  is proportional to  $M_s^2$ .<sup>22</sup> The  $K$  and  $A$  determine the  $\delta$  and  $\gamma$ . For uniaxial anisotropy,  $\gamma = 4\sqrt{AK}$  and  $\delta = \sqrt{A/K}$ .<sup>23</sup> The changes with temperature of  $M_s$  and  $H_a$  affect  $H_c$  through  $\gamma$  and  $\delta$ . The average energy per unit volume of the domain wall is proportional to  $\gamma/\delta$ . Therefore, when a pinning defect with volume  $V$  is embedded inside a wall, the domain-wall energy is reduced by an amount proportional to  $V\gamma/\delta$ . Since the interaction range between the pin and a wall is proportional to  $\delta$ , the work done by the external force in unpinning the domain wall is of order of  $f\delta$ , which is equal to the energy lowered by the pinning site. We therefore have the relation

$$f = C \frac{\gamma}{\delta^2}, \quad (3)$$

where  $C$  is a parameter to be fitted. This relation gives the temperature dependence of the maximum pinning force, which is similar to other detailed pinning models.<sup>24–26</sup> Since the change of  $V$  with temperature is negligible compared with the changes of  $\gamma$  and  $\delta$ , Eq. (3) is a valid approximation when the defect is not magnetic or the temperature dependence of its properties is correlated with those of the matrix.

When the specific energy  $\gamma$  is finite, the pinned domain wall will bow out in external field.<sup>18</sup> It has been observed that in MnBi LTP, the domains form a straight strip pattern when the observation plane is parallel to the  $c$  axis of the LTP crystal, but form a rickrack pattern when the plane is vertical to the  $c$  axis.<sup>27–29</sup> Hence, the bowing is expected to be anisotropic. From the scaling theory<sup>18</sup> for a wall of anisotropic rigidity, the coercive field excluding thermal activation,  $H_0$ , is<sup>18,19</sup>

$$H_0 = \text{const} \frac{\rho^{4/3} f^{8/3} \delta^{1/3}}{M_s \gamma^{5/3}} (8\pi M_s^2 \delta / \gamma)^{-2/3}, \quad (4)$$

where  $\rho$  is the density of pinning sites.

Gaunt<sup>20,21</sup> considered the thermal activated unpinning of a domain wall, and developed a weak pinning model for the coercive field:<sup>20,21</sup>

$$H_c = \frac{F}{2M_s} \left[ 1 - \frac{25k_B T}{31\gamma b^2} \right], \quad (5)$$

where  $b$  is the interaction range of a pinning site and is proportional to  $\delta$ ,  $F$  is the maximum pinning force per unit area of domain-wall.

According to Gaunt<sup>20</sup>, Eq. (4) corresponds to the weak pinning model without considering thermal activation. Therefore, Eq. (5) should reduce to Eq. (4) when  $T$  is small, and the present hybrid model is formed by replacing  $F/2M_s$  in Eq. (5) with  $H_0$  of Eq. (4). Both the intrinsic and the thermal active contributions to  $H_c(T)$  are thus incorporated into the single pinning model, which can be fitted to the measured coercivity.

Equations (1)–(5) are used in fitting, and the fitted result is shown by the solid line in Fig. 8. The good fit strongly suggests that only one pinning mechanism accounts for the coercivity over the entire temperature range. The thermal activation factor is found to be about 66.3% at 600 K, showing that thermal activation has reduced the coercivity by one-third at that temperature. The interaction range  $b$  thus obtained is approximately equal to  $\delta$ . This value is of the right order of magnitude, for a simple estimate gives  $b$  the value of one-fourth of the wall thickness, which is  $0.8\delta$ . The resultant  $\delta$  and  $\gamma$  are shown in Fig. 9.  $\delta$  drops monotonically from 49 Å at 140 K to 14 Å at 600 K. The thin wall at high temperature is responsible for the decrease in  $M_s$  and the increase in  $H_a$ .  $\gamma$  varies between 8.8 and 16.3 ergs/cm<sup>2</sup> with a maximum value at 370 K. At 300 K,  $\gamma = 15.6$  ergs/cm<sup>2</sup>, consistent with Dekker's value of  $15 \pm 1$  ergs/cm<sup>2</sup>.<sup>30</sup>

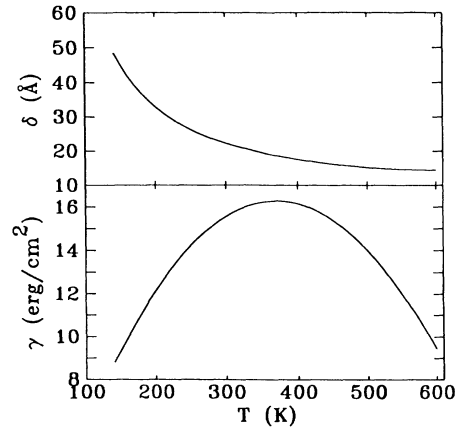


FIG. 9. The domain-wall energy  $\gamma = 4\sqrt{AK}$  and the  $\delta = \sqrt{A/K}$  fitted by the hybrid pinning model using experiment values for  $M_s$  and  $H_a$ .

## IV. CONCLUSION

Using the SPD technique, the anisotropy field  $H_a$  of the low-temperature phase of MnBi has been directly measured for the first time. It is over 6 T at room temperature, and reaches the maximum value of 9 T at 530 K. The anisotropy energy derived from  $H_a$  is consistent with reported data. The saturation magnetization  $M_s$  is also measured by the pulsed field. A fit to the temperature dependence of  $M_s$  suggests a virtual Curie temperature of 775 K. While the reason for the increase in anisotropy at high temperature remains theoretically unresolved, the coercive field  $H_c$  can be well explained over the entire temperature range, by the hybrid domain-wall

pinning model using a single pinning mechanism. The HC phase produced during rapid solidification can be removed by thermal annealing.

## ACKNOWLEDGMENTS

The research was supported by the Natural Sciences and Engineering Research Council of Canada, Fonds pour la Formation de Chercheurs et l'aider à la Recherche, Quebec, and the Faculty of Graduate Studies and Research of McGill University. We thank Mark Sutton for allowing us access to a fitting software, and Dominic Ryan for discussions on improving the electronic circuits.

- 
- <sup>1</sup>Tu Chen and W. Stutius, IEEE Trans. Mag. **MAG - 10**, 581 (1974).  
<sup>2</sup>D. Chen, R. L. Aagard, and T. S. Liu, J. Appl. Phys. **41**, 1395 (1970).  
<sup>3</sup>D. Chen and Y. Gondo, J. Appl. Phys. **35**, 1024 (1964).  
<sup>4</sup>X. Guo, A. Zaluska, Z. Altounian, and J. O. Ström-Olsen, J. Mater. Res. **5**, 2646 (1990).  
<sup>5</sup>G. S. Xu, C. S. Lakshmi, and R. W. Smith, J. Mater. Sci. Lett. **8**, 1113 (1989).  
<sup>6</sup>Y. Allain, J. de Gunzbourg, J. P. Krebs, and A. Miedan-Gros, Rev. Sci. Instrum. **39**, 1360 (1968).  
<sup>7</sup>G. Asti and S. Rinaldi, Phys. Rev. Lett. **28**, 1584 (1972).  
<sup>8</sup>B. W. Roberts, Phys. Rev. **104**, 607 (1956).  
<sup>9</sup>R. R. Heikes, Phys. Rev. **99**, 446 (1955).  
<sup>10</sup>J. Callaway, *Quantum Theory of the Solid State* (Academic, New York, 1976) p. 158.  
<sup>11</sup>W. Stutius, T. Chen, and T. R. Sandin, in *Thermal Expansion—1973 (Boston)*, Proceedings of the 19th Annual Conference on Magnetism and Magnetic Materials, AIP Conf. Proc. No. 17, edited by R. E. Taylor and G. L. Denman (AIP, New York, 1974), p. 1222.  
<sup>12</sup>T. Hihara and Y. Koi, J. Phys. Soc. Jpn. **29**, 343 (1970).  
<sup>13</sup>G. Asti and F. Bolzoni, J. Magn. Mater. **20**, 29 (1980).  
<sup>14</sup>M. R. Notis, D. Shah, C. D. Graham, Jr., and S. R. Trout, J. Appl. Phys. **49**, 2043 (1978).  
<sup>15</sup>R. Pirich, D. Larson, and G. Busch, IEEE Trans. Mag. **MAG-15**, 1754 (1979).  
<sup>16</sup>R. Pirich, IEEE Trans. Mag. **MAG-16**, 1065 (1980).  
<sup>17</sup>A. H. Morrish, *The Physical Principles of Magnetism* (Wiley, New York, 1965).  
<sup>18</sup>H.-R. Hilzinger, Philos. Mag. **36**, 225 (1977).  
<sup>19</sup>H.-R. Hilzinger and H. Kronmüller, Physica B&C **86**, 1365 (1977).  
<sup>20</sup>P. Gaunt, Philos. Mag. B **50**, L45 (1984).  
<sup>21</sup>P. Gaunt, Philos. Mag. B **48**, 261 (1983).  
<sup>22</sup>E. C. Stoner, F. R. S., and E. P. Wohlfarth, Philos. Trans. R. Soc. London, Ser. A **240**, 599 (1948).  
<sup>23</sup>S. Chikazumi, *Physics of Magnetism* (Wiley, New York, 1964).  
<sup>24</sup>D. I. Paul, Phys. Lett. **64A**, 485 (1977).  
<sup>25</sup>X. Chen and P. Gaunt, J. Appl. Phys. **67**, 2540 (1990).  
<sup>26</sup>X. Chen and P. Gaunt, J. Appl. Phys. **67**, 4592 (1990).  
<sup>27</sup>Ya. S. Sher, E. V. Shtol'ts, and V. I. Margolina, Zh. Eksp. Teor. Fiz. **38**, 46 (1960) [Sov. Phys. JETP **11**, 33 (1960)].  
<sup>28</sup>B. W. Roberts and C. P. Bean, Phys. Rev. **96**, 1494 (1954).  
<sup>29</sup>S. Honda, S. Konishi, and T. Kusuda, Appl. Phys. Lett. **22**, 421 (1972).  
<sup>30</sup>P. Dekker, J. Magn. Mater. **2**, 32 (1976).